

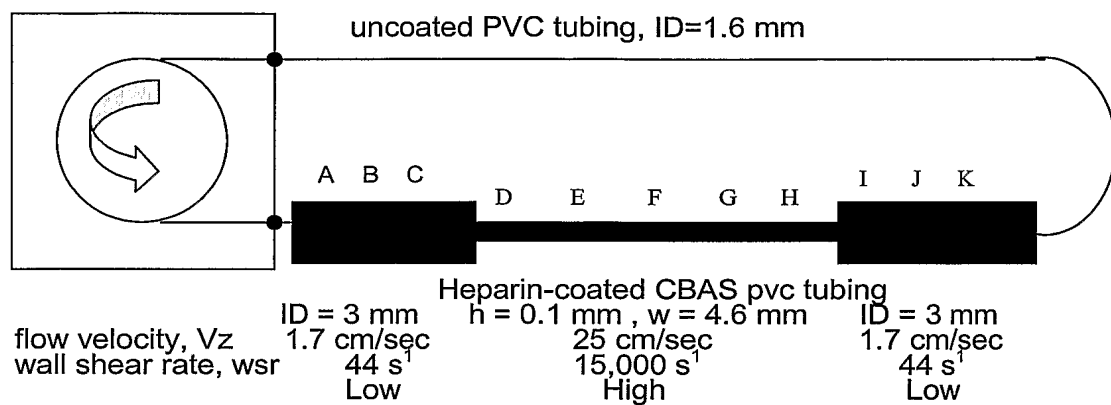
FIG. 1**IN VITRO FLOW MODEL**

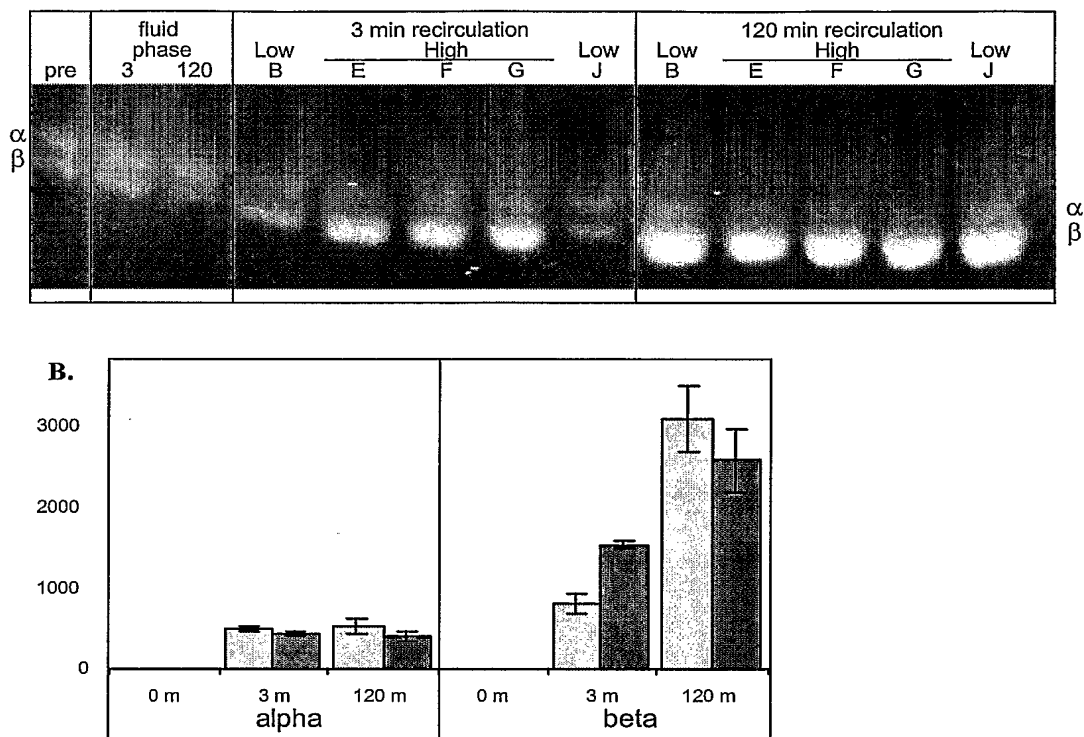
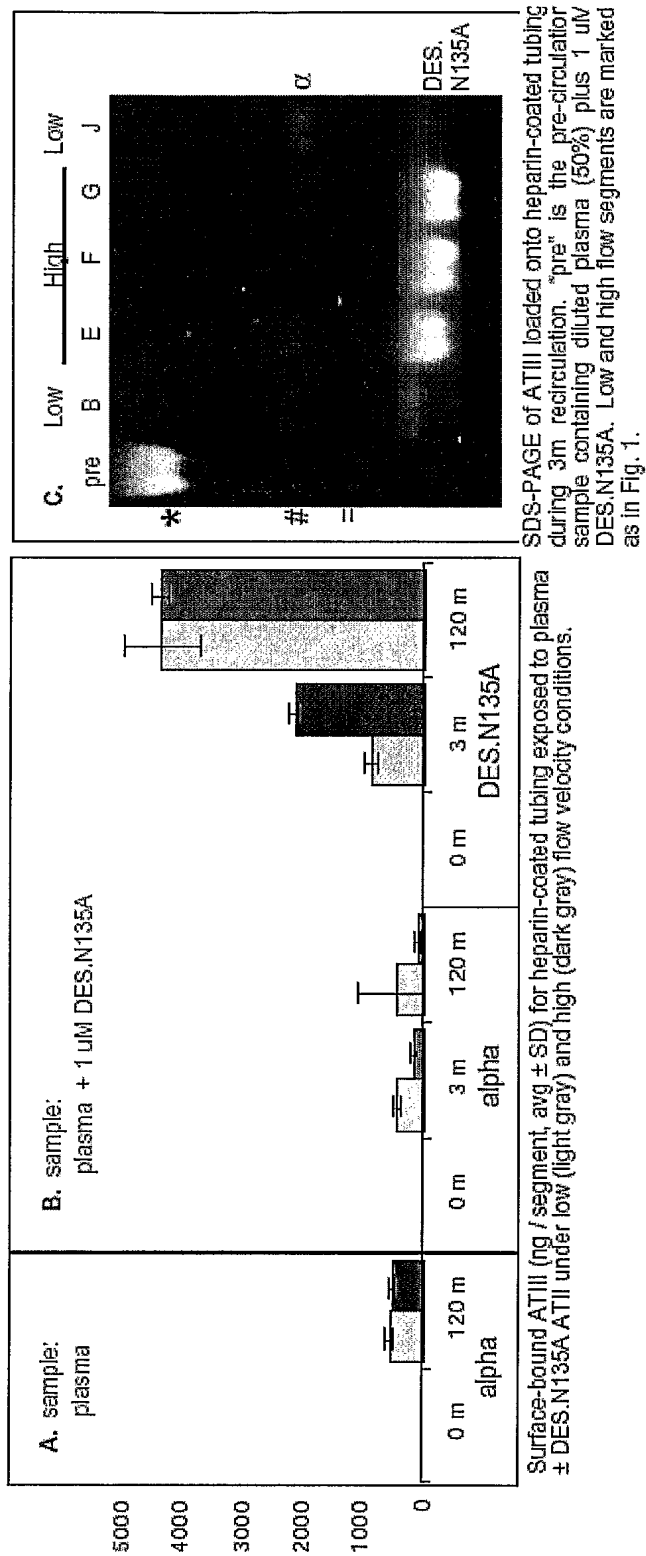
FIG. 2

FIG. 3



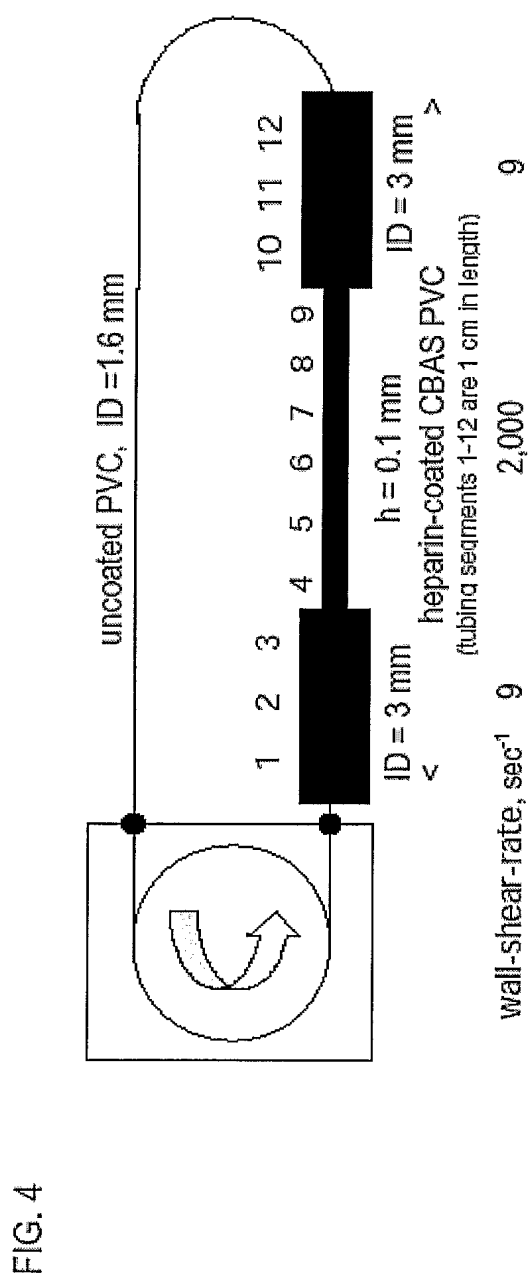
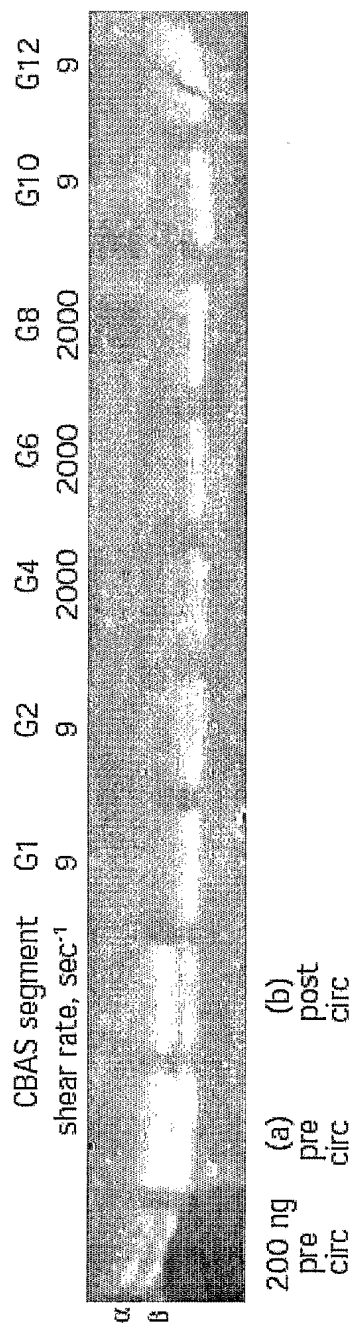


FIG. 5



6
EIG

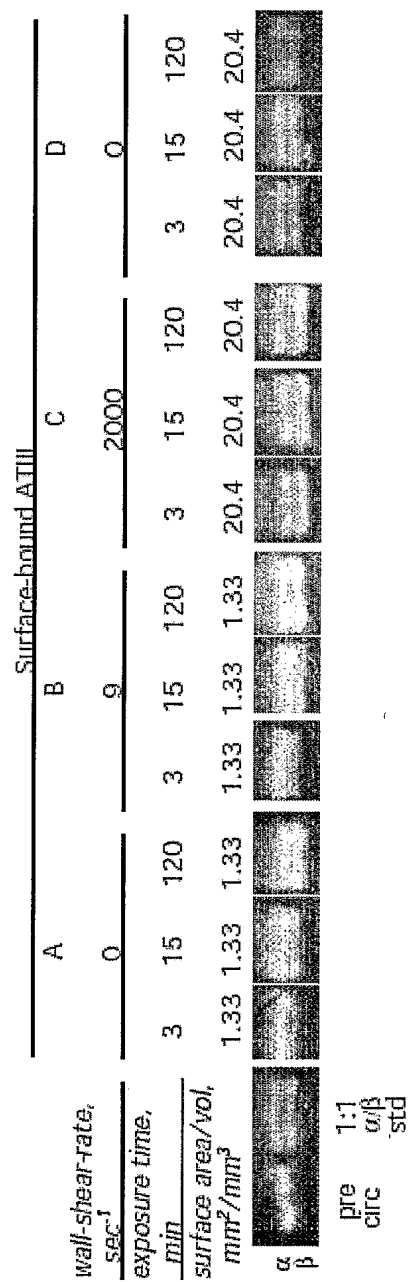


FIG. 7

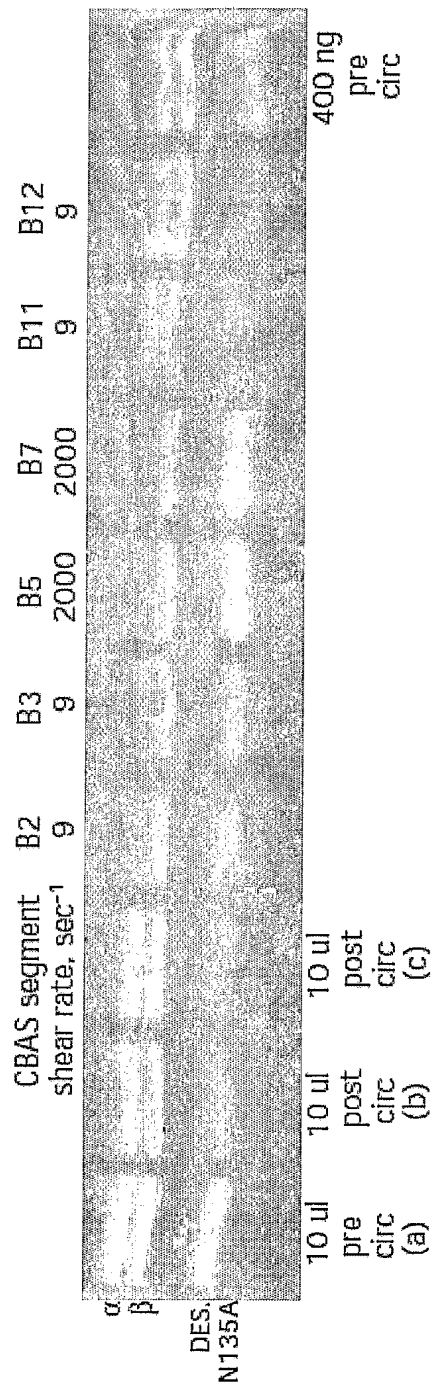


FIG. 8

IN VITRO FLOW MODEL

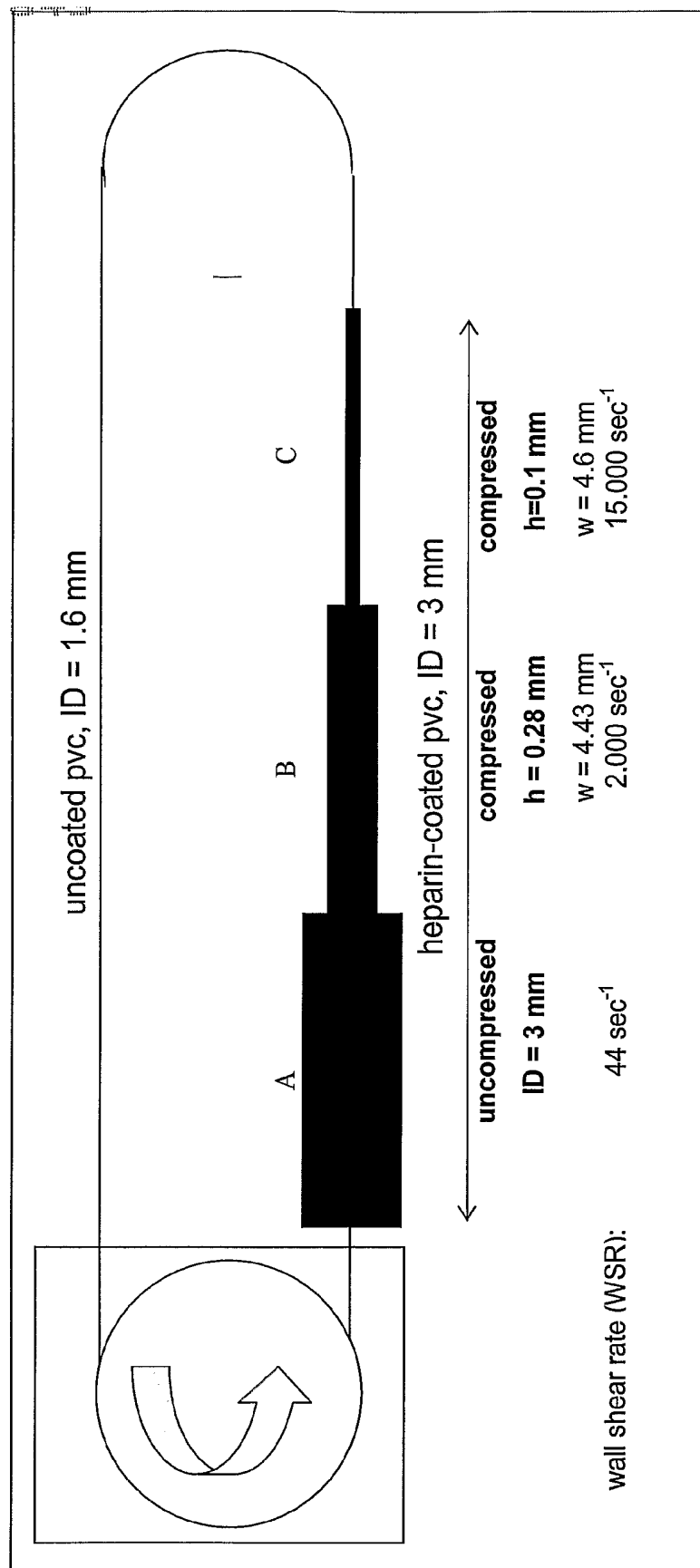


FIG. 9 Panel A

A. WALL SHEAR RATE – DEPENDENT DIFFERENTIAL BINDING OF ATIII ISOFORMS TO HEPARIN-COATED SURFACES

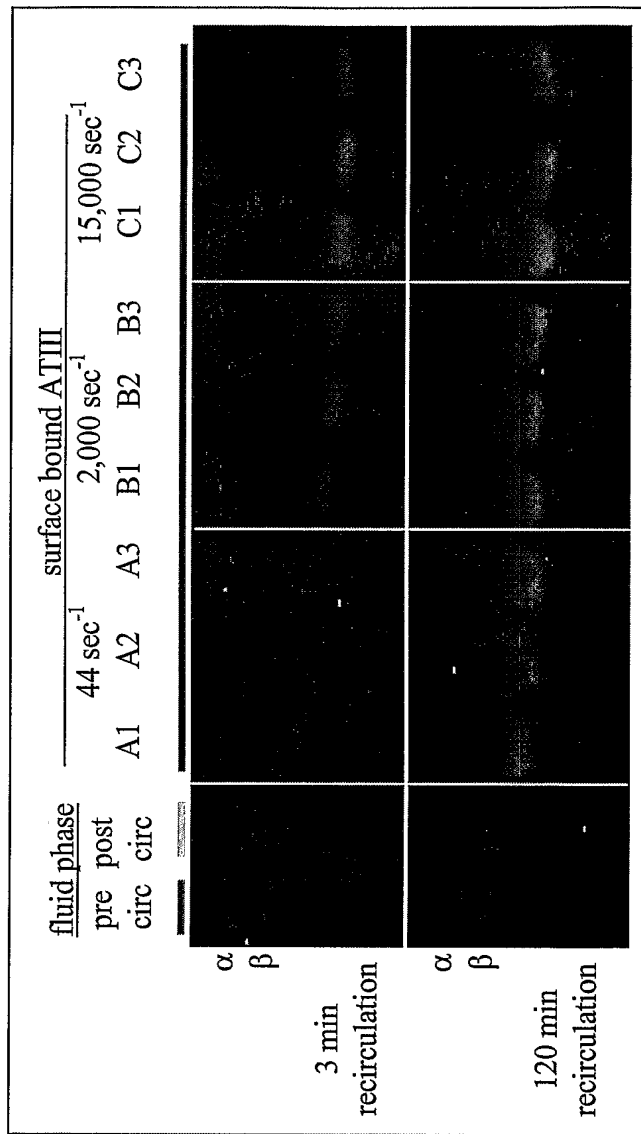


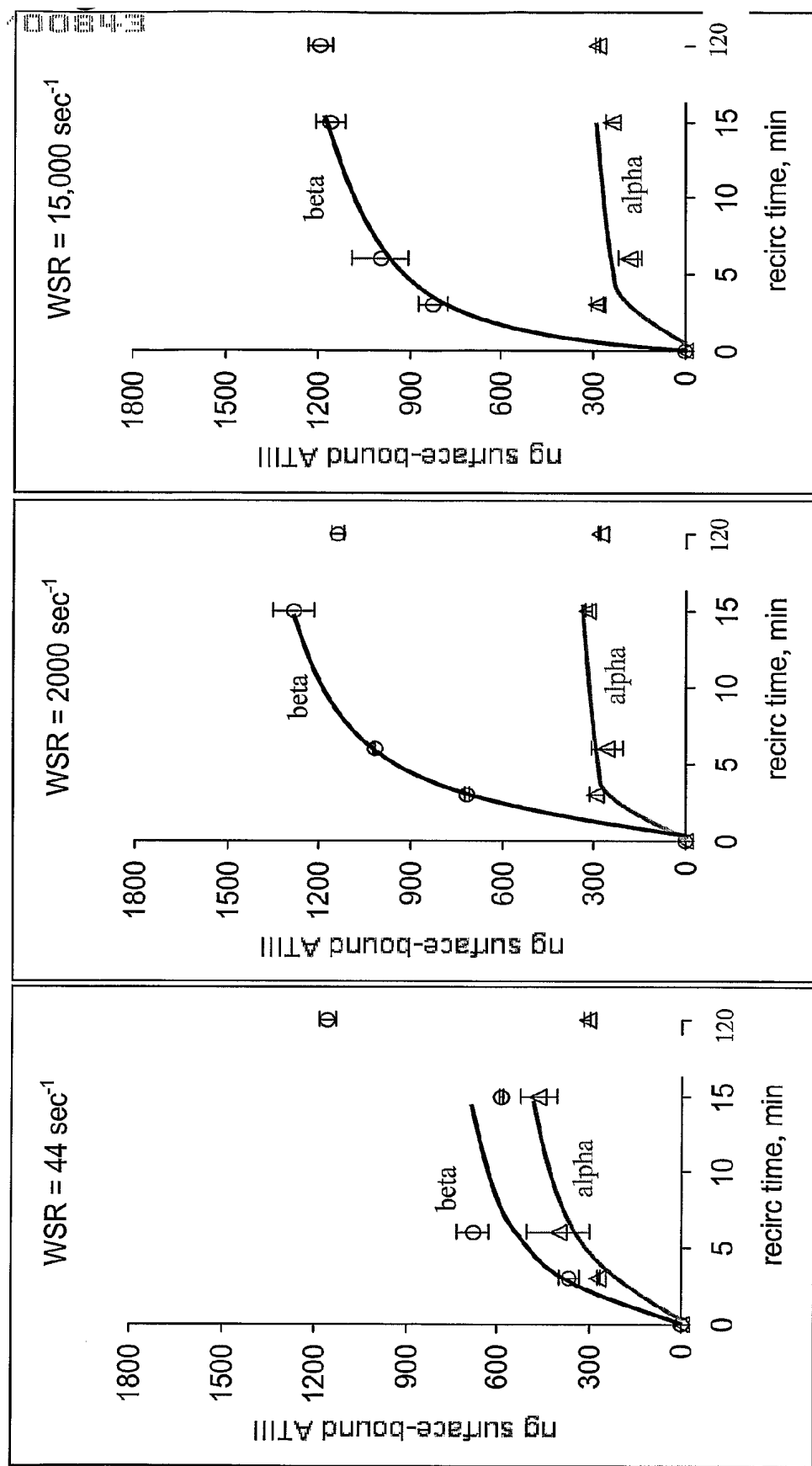
Fig. 9 Panel B

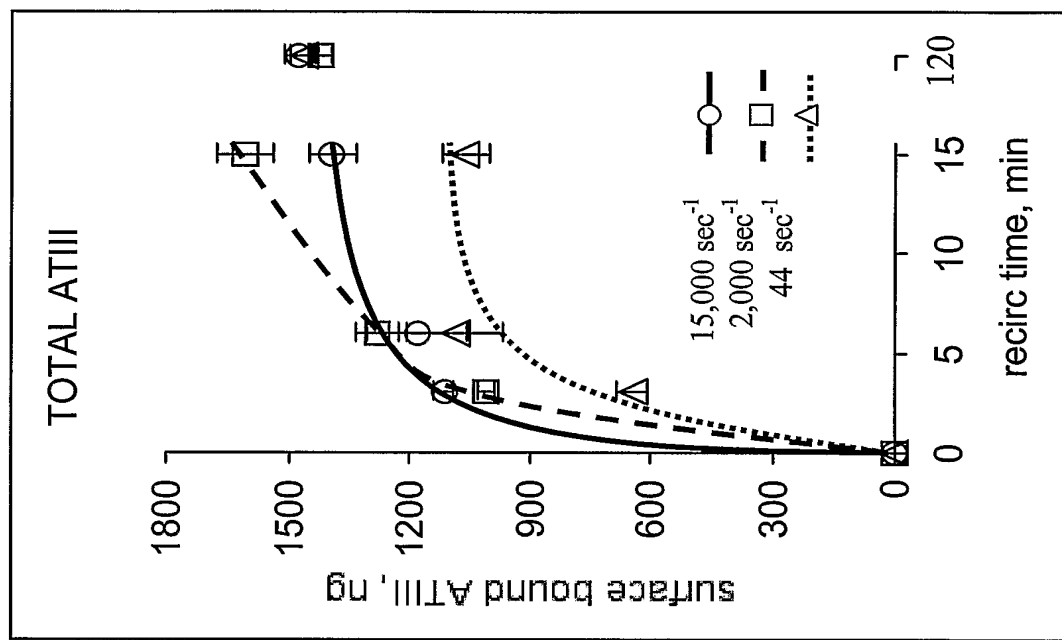
Fig. 9 Panel C

Fig. 10 Panel A

RECOMBINANT DES.N135A ATIII LOADS ONTO HEPARIN-COATED BIOMATERIAL SURFACES MORE EFFICIENTLY THAN ENDOGENOUS PLASMA ATIIIS

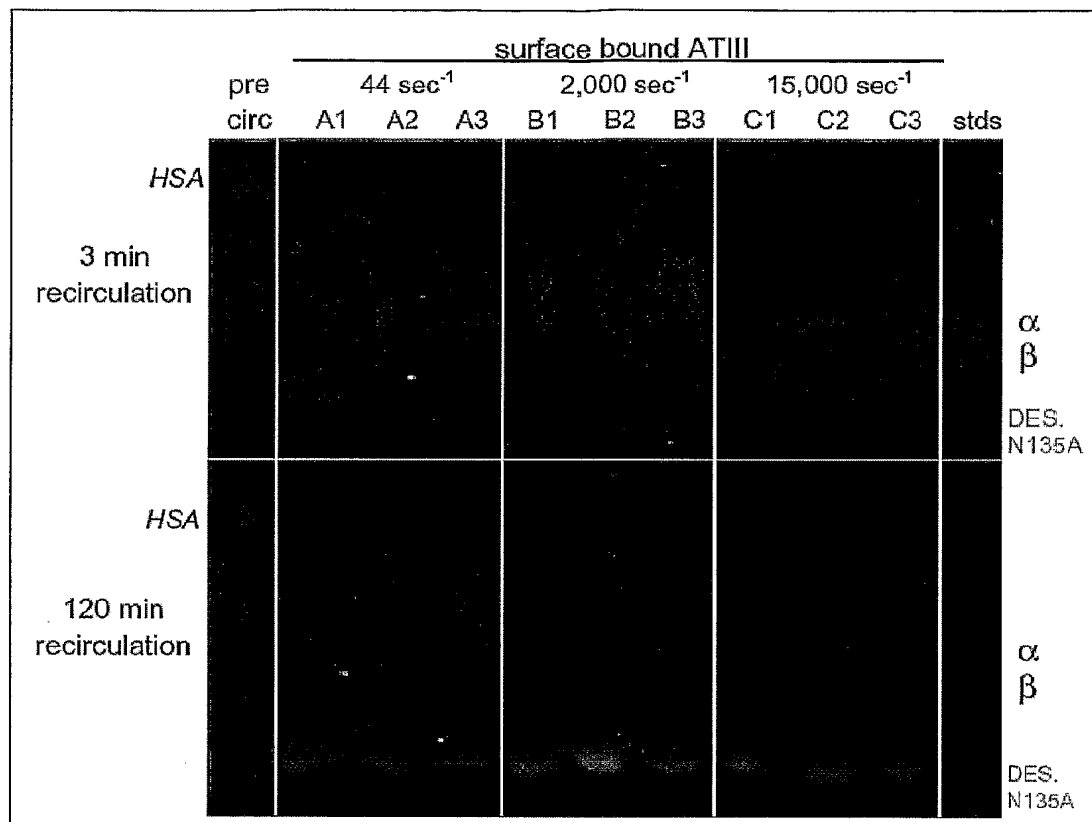


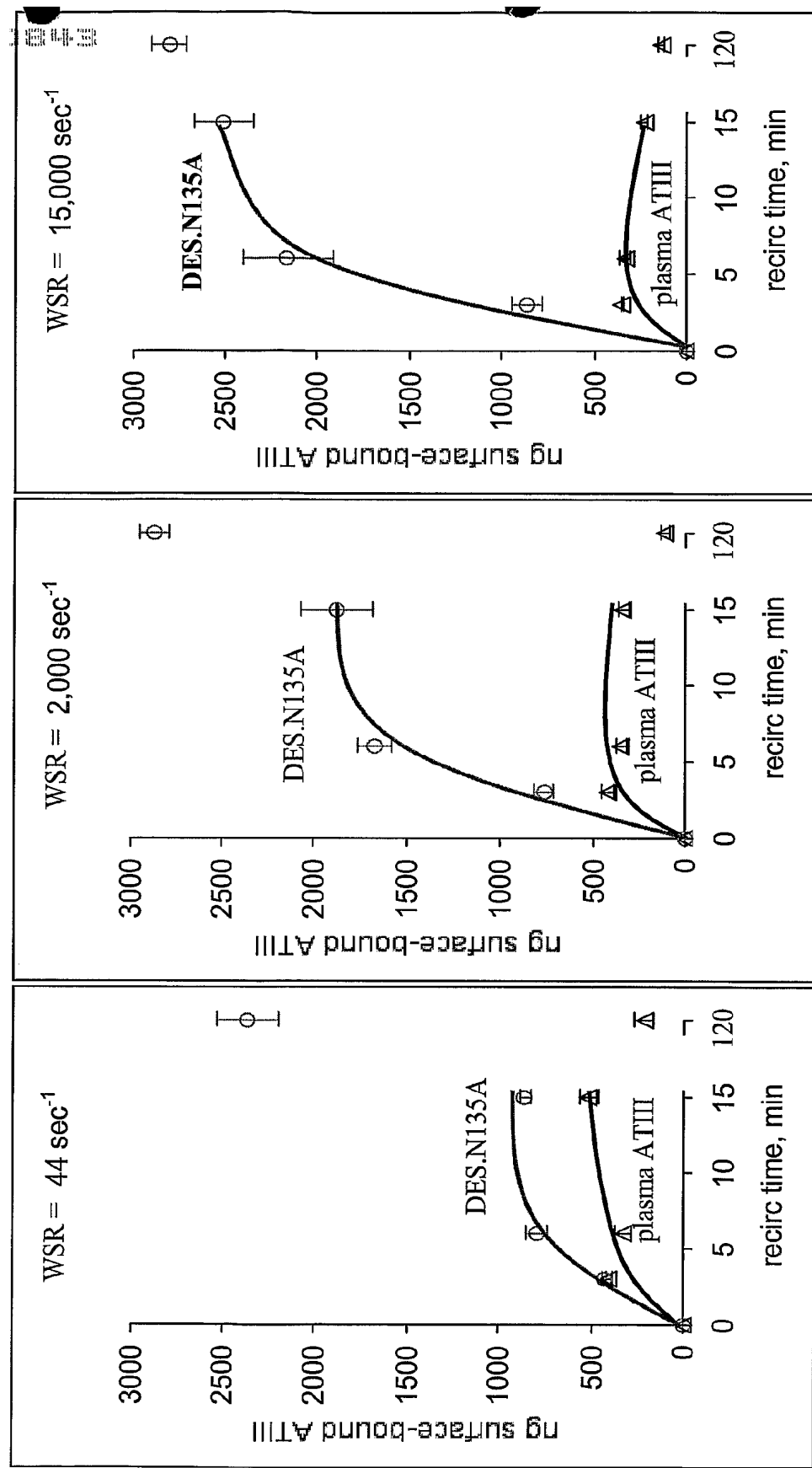
Fig. 10 Panel B

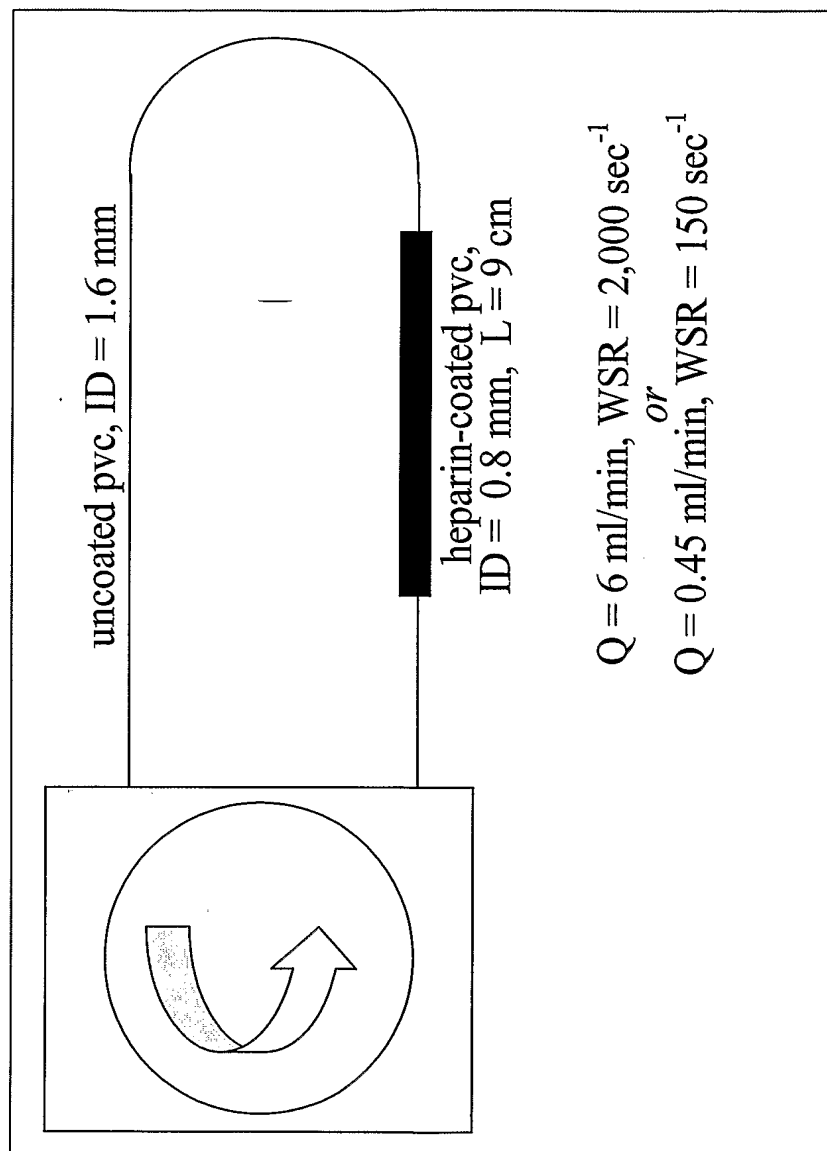
FIG. 11 Panel A**FUNCTIONAL INHIBITION OF FLOWING THROMBIN BY
SURFACE-TARGETED ATIIIs**

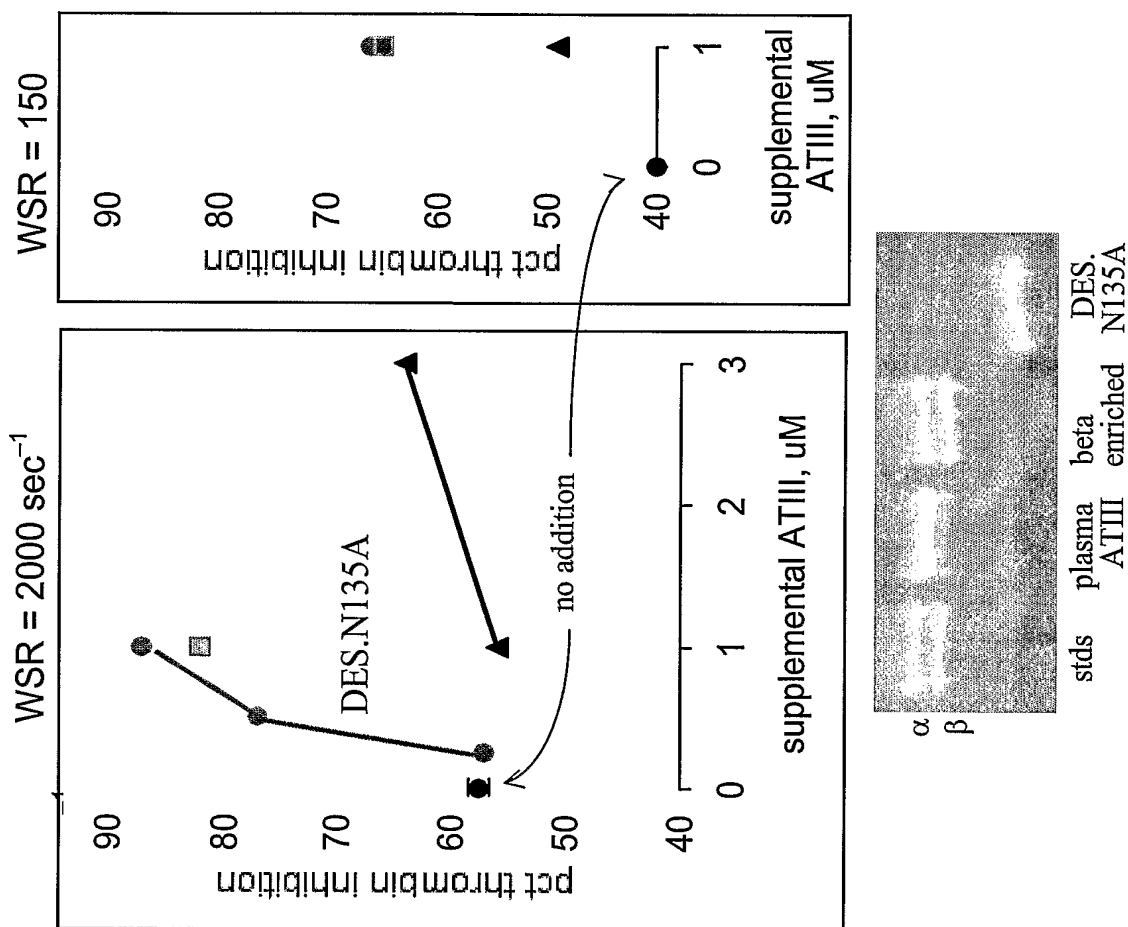
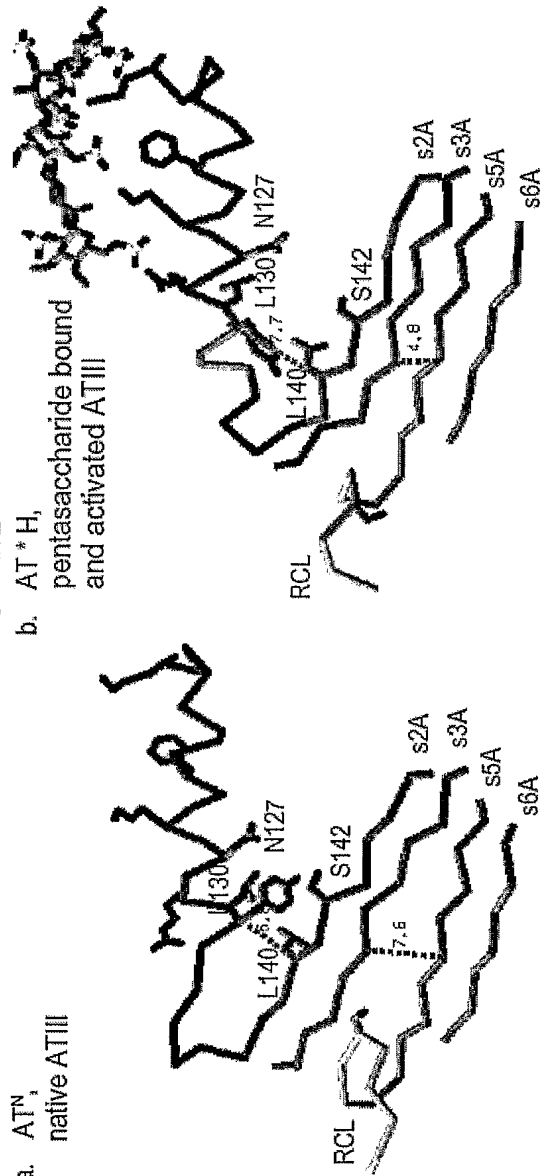
FIG. 11 Panel B

FIG. 12

c.

Tyrosine-131 distal ring carbon interactions with helix D and strand 2A residues in native and pentasaccharide-activated AT^{II} s, \AA

		AT^N (1E05i)	$\text{AT}^* \text{H}$ (1E03i)
Y131	CE1	-	S142
Y131	CE1	-	L140
Y131	CE1	-	L130
Y131	CZ	-	L130
Y131	CZ	-	L130
Y131	CZ	-	S142
Y131	CE2	-	L130
Y131	CE2	-	L130
Y131	CE2	-	N127
Y131	CE2	-	N127
Y131	CE2	-	S142

FIG. 13